

Influence of perovskite termination on oxide heteroepitaxy

D. A. Schmidt^{a)}

*Department of Physics, University of Washington, Seattle, Washington 98195-1560
and Center for Nanotechnology, University of Washington, Seattle, Washington 98195-1560*

Taisuke Ohta^{b)}

*Department of Material Science and Engineering, University of Washington, Seattle,
Washington 98195-2120 and Center for Nanotechnology, University of Washington, Seattle,
Washington 98195-1560*

Q. Yu^{c)}

Department of Physics, University of Washington, Seattle, Washington 98195-1560

Marjorie A. Olmstead

*Department of Physics, University of Washington, Seattle, Washington 98195-1560
and Center for Nanotechnology, University of Washington, Seattle, Washington 98195-1560*

(Received 18 August 2005; accepted 11 April 2006; published online 12 June 2006)

We report a combined high-temperature scanning tunneling microscopy, ion scattering spectroscopy, and photoelectron spectroscopy study of bare lanthanum aluminate [LaAlO₃(LAO)] and of the initial stages of anatase TiO₂ growth on LAO(001). LAO(001) exhibits mixed La–O and Al–O₂ surface terminations at 400 °C. Heteroepitaxial TiO₂, grown by evaporating Ti metal in O₂, nucleates near step edges, growing out to cover both upper and lower terraces uniformly, regardless of termination, indicating that the substrate cations and perovskite surface polarity play little direct role in controlling the morphology of this single-metal oxide heteroepitaxy. TiO₂ films of 1.5 nm in thickness exhibit a surface reconstruction similar to the bulk anatase (1 × 4). © 2006 American Institute of Physics. [DOI: 10.1063/1.2202197]

I. INTRODUCTION

The alternating layer structure of LaAlO₃(001), a commonly used substrate for growth of high T_c superconductors^{1–4} and other perovskite-based materials,⁵ raises interesting questions about the role of substrate cations and polarity in oxide heteroepitaxy. Depending on temperature and surface preparation, LaAlO₃(001) surfaces may exhibit single-height ($d=1.89$ Å) steps separating terraces of alternating La–O and AlO₂ terminations, double-height ($2d$) steps between terraces of the same termination, or combinations thereof. The two terminations differ in their nominal charge: La³⁺O²⁻=(La–O)⁺ and Al³⁺(O²⁻)₂=(Al–O₂)⁻. In growth of SrTiO₃ (STO) on LaAlO₃ (LAO) (Ref. 5) and vice versa,⁶ the interface is believed to be either (Ti–O₂)⁰/(La–O)⁺ or (Sr–O)⁰/(Al–O₂)⁻, which would result in an excess 0.5 electron or hole, respectively, per interface unit cell. Mixed valence Ti^{3+/4+} at a (Ti–O₂)⁰/(La–O)⁺ interface accommodates this charge mismatch, leading to a stable interface with trapped electrons;⁶ (Sr–O)⁰/(Al–O₂)⁻ on the other hand is insulating with numerous defects.^{5,6}

Anatase TiO₂ is lattice matched to LAO (3.79 Å vs 3.78 Å at room temperature); the neutral TiO₂ layer is buckled (unlike STO), and alternate layers change orientation rather than cation or polarity. Different interface structures and charges might be expected when TiO₂ is deposited on

La–O or Al–O₂ terminated LAO. The spacing between low energy sites for positive and negative ions is $\sqrt{2}$ larger on the Al–O₂ termination than on La–O. Also, while the excess charge for the La–O termination may be absorbed by mixed valence Ti^{3+/4+}, similar to STO/LAO, the most likely candidates for balancing the excess charge of Al–O₂ termination are oxygen vacancies and exchange of Ti⁴⁺ with substrate Al³⁺. Growth on Al–O₂ terminated regions might thus involve nonwetting, interdiffused, or oxygen deficient interfaces, perhaps accompanied by defect formation. Technological interest in growth of laminar, ≥ 10 nm thick anatase films on LAO (Refs. 7–11) for spintronic applications raises the question of whether the interface properties may be optimized by controlling the LAO surface termination.

Previous studies^{5,12–15} have indicated that LAO(001) is terminated with Al–O₂ at room temperature, switching to La–O above ~ 250 °C; more recent studies¹⁶ report both terminations at room temperature but only La–O at temperatures above 727 °C. In this paper, we report growth of the single-metal oxide TiO₂ on LAO surfaces prepared with roughly equal populations of La–O and Al–O₂ interspersed on the scale of several nanometers. Investigations with ion scattering spectroscopy (ISS), x-ray photoemission spectroscopy (XPS), and scanning tunneling microscopy (STM) surprisingly show no significant differences in TiO₂ nucleation and growth on the two terminations. Rather, TiO₂ nucleates at step edges and grows outward from single-height steps on both the upper and lower terraces, covering both La–O and Al–O₂ terraces uniformly before extensive nucleation of a

^{a)}Present address: International Center for Young Scientists, NIMS, Tsukuba, Japan; electronic mail: schmidt.diedrich@nims.go.jp

^{b)}Present address: Advanced Light Source, Berkeley, CA 94720.

^{c)}Present address: CNT, UW, Seattle, WA 98195-2140.

second layer. When the film is 1.5 nm thick, it shows a multidomain (1×4) TiO_2 surface reconstruction similar to that of crystalline anatase.^{17–20}

II. EXPERIMENTS

Commercially prepared (Princeton Scientific Corp.) LAO substrates were epipolished on one side. Substrates were sonicated in methanol before vacuum coating the non-polished side with a thin metal film (30 nm Ti followed by 90 nm Pt). The LAO was wiped clean with methanol prior to introduction in the ultrahigh vacuum (UHV) system (base pressure $< 1 \times 10^{-10}$ torr). Substrates were then annealed at 670 °C, as measured with an optical pyrometer, in a partial pressure of molecular oxygen ($P_{\text{O}_2} = 5 \times 10^{-5}$ torr, purity $> 99.99\%$) for 25 min. Samples were resistively heated via the metal coating and/or a Si wafer in parallel with the sample. XPS showed the prepared LAO substrates to be free of carbon and other residual contaminants within an experimental resolution of 0.05 ML (monolayer).

Thin (≤ 1.5 nm) anatase TiO_2 films were deposited by molecular beam epitaxy (MBE). Pure ($> 99.99\%$) Ti metal was evaporated from an electron-beam evaporator in a background of O_2 at $P_{\text{O}_2} = 5 \times 10^{-5}$ torr at a substrate temperature $T_{\text{sub}} = 570$ °C. A growth rate of $1 \text{ \AA}/\text{min}$ was measured by a water-cooled quartz crystal monitor. After growth, T_{sub} was lowered to 300 °C in the presence of molecular oxygen to suppress oxygen vacancy formation. The oxygen was then evacuated while the sample was cooled to room temperature. The samples were then transferred under UHV to separate analyses [ISS, low-energy electron diffraction (LEED), and XPS] and STM chambers. Film thickness estimates using XPS intensities from laminar films were consistent with those estimated from the quartz crystal monitor.

Core-level photoemission (XPS) was excited with a Mg $K\alpha$ x-ray source. ISS was used to determine the surface elemental composition. The 500–1000 eV He^+ ions utilized yield sensitivity to only the exposed surface layer. To alleviate surface charging, as well as to probe the double-metal surface termination under growthlike conditions, elevated substrate temperatures of $T_{\text{sub}} = 400$ °C were utilized for STM and ISS on the insulating bare LAO and submonolayer TiO_2 samples. For Fig. 2(c), a temperature of $T_{\text{sub}} = 60$ °C (measured by thermocouple) was required for this small-scale imaging of a four to five molecular layer thick film, while large-scale STM [Fig. 1(c)] was obtained at room temperature. All STM bias voltages are measured with respect to a grounded sample.

III. RESULTS

A. Surface morphology of annealed LAO

The large-scale surface morphology of oxygen-annealed LAO(001) before deposition of TiO_2 is shown in Fig. 1(a). The bare, oxygen-annealed LAO(001) surface, imaged with high-temperature STM (HT-STM) at 400 °C, consists of long, ~ 150 nm wide regions [labeled I and II in Fig. 1(a)] that have average heights differing by ~ 0.4 nm or one LAO unit cell. This implies that the base level on each terrace

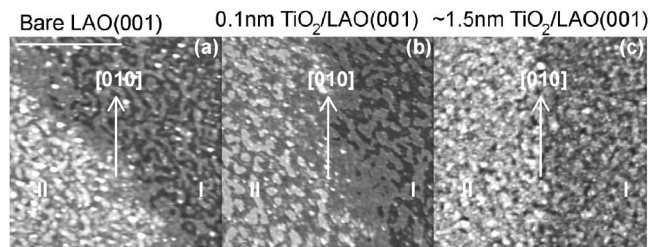


FIG. 1. Large-scale surface morphology of LAO(001) before and after deposition of TiO_2 . $200 \times 200 \text{ nm}^2$ STM images of (a) bare LAO(001) annealed in $5 \times 10^{-5} \text{ O}_2$ at 670 °C, (b) ~ 0.1 nm (~ 0.5 ML) TiO_2 deposited at 570 °C on postannealed LAO(001), and (c) ~ 1.5 nm TiO_2 deposited at 570 °C on postannealed LAO(001). Regions marked I and II in (a)–(c) have average heights differing by ~ 0.4 nm, consistent with the 0.37 nm LAO unit cell height. Scale bare in (a) is 100 nm. Image conditions: [(a) and (b)] $T_{\text{sub}} = 400$ °C, 4.5 V, 0.08 nA; (c) $T_{\text{sub}} = \text{room temperature}$, 2.1 V, 0.198 nA.

consists of the same termination (La-O or Al-O_2). Room temperature, noncontact atomic force microscopy (nc-AFM) of similarly prepared samples (not shown) reveals just this global step/terrace structure, with a mottled appearance on the terraces. The HT-STM results in Fig. 1(a) clearly show that the terraces are neither atomically flat nor consisting of a single metal-oxide termination; rather, snakelike islands ~ 10 – 20 nm in width and up to ~ 40 nm in length are interspersed across the terraces. The result is a terrace consisting of a single, base surface termination with islands of possibly differing surface termination, depending on their height: “single-height” steps of height $d = 1.89 \text{ \AA}$, or half the LAO unit cell, should alternate surface terminations, while “double-height” steps of height $2d$ separate terraces with the same La-O or Al-O_2 termination (see Fig. 4). Figure 2(a) shows a high resolution image of the border between regions I and II seen in Fig. 1(a), with solid white lines highlighting some steps of height $2d$ and dotted lines highlighting some single-height steps. The cross section along the line A–A' [Fig. 2(d)] shows numerous islands of height d and occasionally $2d$ scattered throughout, implying that the surface has both La-O and Al-O_2 sublattices exposed. Surface termination by both cations was confirmed by ISS measurements of the surface elemental composition, also at 400 °C, which indicated the presence of O, La, and Al at the surface (and no other atomic species).

B. Nucleation and growth of anatase TiO_2 on LAO(001)

Deposition of ~ 0.5 molecular layers of TiO_2 on LAO(001) at 570 °C does not significantly alter the large-scale surface morphology of the bare LAO [compare Figs. 1(a) and 1(b)]: both show long terrace regions of average height difference $2d$, with smaller scale islands primarily of height d dispersed throughout. At smaller length scales [Fig. 2(b)], the nucleation of this submonolayer TiO_2 film may be seen. TiO_2 growth is seen both on the base of the terrace and on the islands [dotted white lines in Fig. 2(b) highlight some single step height edges]. Darker regions near the centers of both island and terrace regions likely correspond to uncovered LAO, indicating that the TiO_2 nucleates at steps and grows out to cover either terrace or island [solid white lines

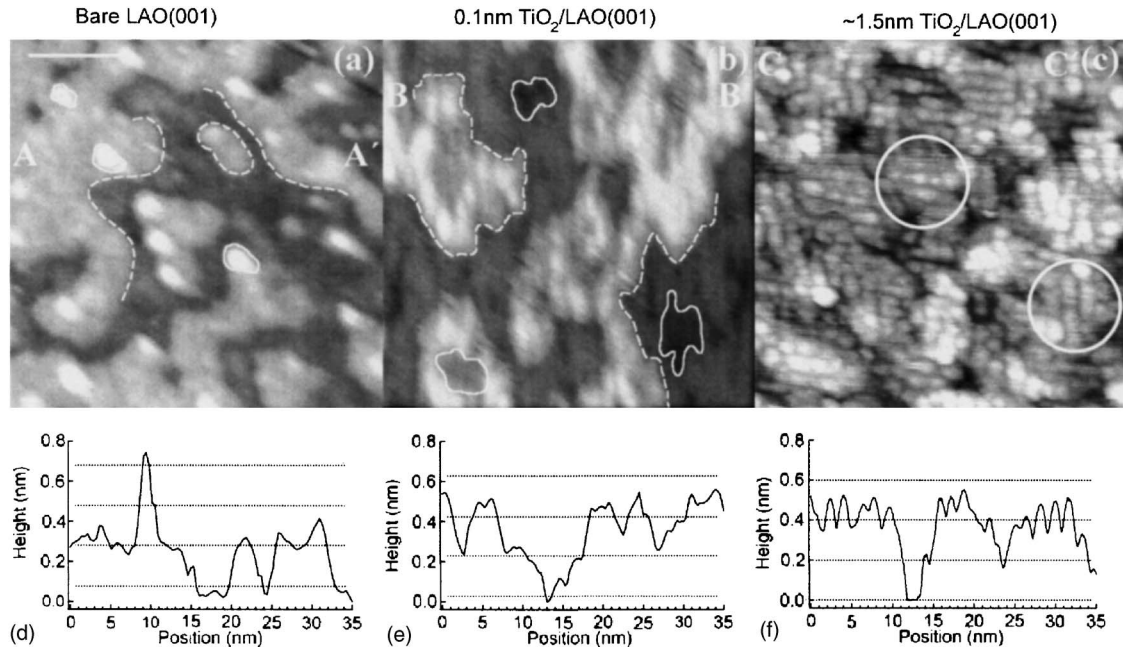


FIG. 2. High resolution surface morphology of LAO(001) before and after deposition of 1.5 nm TiO_2 . $35 \times 35 \text{ nm}^2$ STM images of (a) bare LAO(001) annealed in $5 \times 10^{-5} \text{ O}_2$ at 670°C , (b) $\sim 0.1 \text{ nm}$ ($\sim 0.5 \text{ ML}$) TiO_2 deposited at 570°C on postannealed LAO(001), and (c) $\sim 1.5 \text{ nm}$ TiO_2 deposited at 570°C on postannealed LAO(001). [(d)–(f)] height vs position along line connecting the capital letters in (a)–(c). Horizontal dotted lines in (d)–(f) are single-step heights in LAO(001). Dashed white lines in (a) and (b) highlight some single-height (0.2 nm) steps, while in (b) highlight regions of no TiO_2 coverage. The circles in (c) indicate two domains of the 1×4 TiO_2 surface reconstruction, rotated by 90° . Scale bar in (a) is 10 nm. Images (a)–(c) have same orientation as those in Figs. 1(a)–1(c). Image conditions: [(a) and (b)] $T_{\text{sub}}=400^\circ\text{C}$, 4.5 V, 0.08 nA; (c) $T_{\text{sub}}=60^\circ\text{C}$, 4 V, 0.16 nA.

in Fig. 2(b)]. For example, Fig. 2(e), which depicts the cross section along the line connecting points B and B', shows growth across the terrace except areas which tend to be far from the step edges (region between ~ 11 and ~ 16 nm). The predominance of steps of height d indicates similar monolayer-high islands of TiO_2 on both La–O and Al–O₂ surface terminations. ISS showed partial coverage of both surface terminations, with reduced, but still measurable, scattering from both Al and La, in addition to O and Ti. No large-scale second-layer TiO_2 nucleation is observed before the first layer coalesces.

Continued growth of TiO_2 results in fairly uniform coverage of the substrate, with predominantly single-height steps after about four to five molecular layers of deposition [Fig. 1(c)]. Again, distinct, $\sim 150 \text{ nm}$ wide terraces separated in height by $2d$ are observed in the larger scale image [Fig. 1(c)]; the edges are more clearly aligned with the [010] direction than for the bare LAO [Fig. 1(a)] or initial growth [Fig. 1(b)]. This may be a result of the lower measurement temperature (room temperature versus 400°C), individual sample differences in miscut angle, or the TiO_2 growth itself.

High resolution STM [Fig. 2(c)] shows that the $\text{TiO}_2(001)$ film exhibits ~ 8 – 10 nm diameter domains containing bright rows in groups of 3 or 4 oriented along either [100] or [010]. The observed ~ 1.8 – 2 nm spacing between rows is within our calibration error in this variable-temperature experiment of the 1.6 nm spacing of the well-studied 1×4 reconstruction of anatase (001).^{17–20} A similar morphology containing small domains in both [100] and [010] orientations is seen for anatase films grown on SrTiO_3 .^{18,20} However, we observe an additional modulation

of the rows in the perpendicular direction, also with a length scale on the order of 2 nm. Of significant importance in Fig. 2(c) is the uniformity in coverage of the LAO by the TiO_2 film, confirming TiO_2 nucleation on both surface terminations of LAO(001). The height variations along the line connecting points C and C' [Fig. 2(f)] show multiple step heights, combining the $d_{\text{LAO}}=0.19 \text{ nm}$ step of the substrate, the $d_{\text{TiO}_2}=0.24 \text{ nm}$ layer spacing in the anatase film, plus the additional corrugation of the surface reconstruction.

Figures 3(a)–3(c) show Ti $2p$ photoemission using Mg $K\alpha$ radiation. The first two spectra [Figs. 3(a) and 3(b)] are for the same 0.1 and 1.5 nm films as in Figs. 1(b) and 1(c). The last spectrum [Fig. 3(c)] is from a Ti film with the same Ti exposure as for the film in Fig. 1(c), but deposited in the absence of O_2 ($P_{\text{O}_2} < 1 \times 10^{-10} \text{ torr}$). The submonolayer and thicker TiO_2 films both show a distinctive Ti^{4+} oxidation peak at 459 eV binding energy (BE) with no significant contributions from intermediate oxidation states. In contrast to these spectra, the Ti metal XPS shows multiple Ti oxidation states, with roughly half the Ti in oxidized Ti^{3+} and Ti^{4+} states and with the other half remaining as metallic Ti^0 . The dashed and dotted curves in Figs. 3(a)–3(c) are the individual peak-fit lines for the Ti $2p_{3/2}$ and $2p_{1/2}$ states, respectively. The additional peaks at 458, 461, and 466 eV (dotted curves) in Fig. 3(c) are the Ti $2p_{1/2}$ spin-orbit peak from the Ti^{0+} , Ti^{3+} , and Ti^{4+} oxidation states, respectively.

The crystal phase of TiO_2 films grown under similar conditions to those for which data are presented here was verified to be anatase using the soft x-ray absorption near edge structure (XANES) of the Ti L edge and O K edge (data

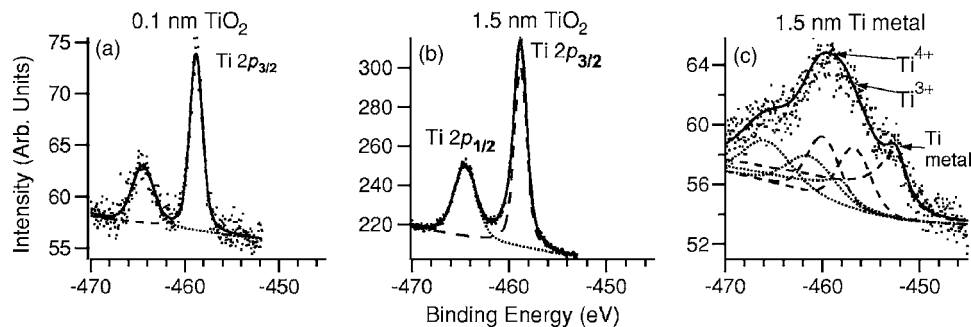


FIG. 3. Ti $2p$ core-level x-ray photoelectron spectroscopy. Ti $2p$ XPS spectra of (a) 0.1 nm TiO_2 , (b) 1.5 nm TiO_2 , and (c) 1.5 nm Ti metal. All XPS spectra were taken *in situ* using $\text{Mg } K\alpha$ radiation. Dots are raw data points, dashed and dotted curves are Ti $2p_{3/2}$ and $2p_{1/2}$ individual peak-fit lines, and solid curves are the summed fits. The additional peaks at 458, 461, and 466 eV (dotted curves) in (c) are the Ti $2p_{1/2}$ spin-orbit peak from the Ti^{0+} , Ti^{3+} , and Ti^{4+} oxidation states, respectively. Growth conditions were identical for (a)–(c), except for (c) where $P_{\text{O}_2} < 1 \times 10^{-10}$ torr. Note the multiple oxidation states of Ti when pure metal is evaporated on LAO(001), (c).

taken at the Advanced Light Source in Berkeley, CA, Beamline 7.0.1). Our XANES results were consistent with previously published data for both bulk anatase^{21–24} and thin film TiO_2 on LAO(001) (Refs. 8 and 11) and distinctly different from our measurements on a rutile standard.

IV. DISCUSSION

We first discuss the high-temperature (400 °C) termination of LAO(001). Our results indicate a base terrace of a single termination, with about half that surface covered by single-height step islands; these islands would be of the opposite termination in the bulk LAO crystal structure. Surfaces covered by a single, unreconstructed $(\text{La}-\text{O})^+$ or $(\text{Al}-\text{O}_2)^-$ termination would be electrostatically unstable due to the uncompensated surface dipole. The simplest way to stabilize the surface is for the surface layer to be half occupied on a scale less than the surface electrostatic screening length. It is unlikely that the observed 10–20 nm scale of the alternating terminations is small enough to fully cancel the dipole, although the insensitivity of nc-AFM to these islands is indicative of a long-range Coulomb interaction of these alternately charged terminations. Alternative solutions for surface charge balance include reconstruction to reduce the surface charge by half, e.g., 1/4 monolayer of oxygen vacancies (for $\text{Al}-\text{O}_2$) or adatoms (for $\text{La}-\text{O}$).

A schematic of LAO(001) with multiple step and terrace configurations is shown in Fig. 4. Our combined STM and ISS results do not distinguish between a $\text{La}-\text{O}$ base with $\text{Al}-\text{O}_2$ islands and vice versa. Since the $(\text{La}-\text{O})^+$ termination can be neutralized by oxygen adsorption, annealing in

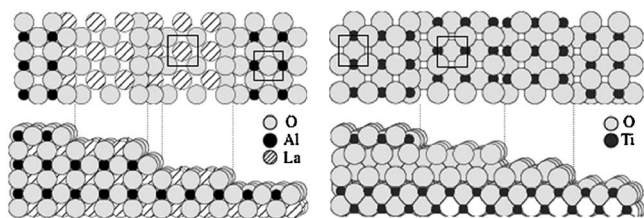


FIG. 4. Schematic of LAO(001) surface termination. Left: LAO(001); right: anatase (001). Bottom: 3D view along the $[010]$ direction, with the spheres having the appropriate ionic radii. Top: Planar view of the stepped (001) surface. Lower levels included only at step edges. Boxes denote 1×1 surface unit cells. Steps are shown in oxygen-rich configuration.

O_2 at 670 °C would favor $\text{La}-\text{O}$ termination; subsequent heating to 400 °C in UHV for imaging could then etch the $\text{La}-\text{O}$, leaving $\text{La}-\text{O}$ islands on an $\text{Al}-\text{O}_2$ base. On the other hand, if the surface starts out as $\text{Al}-\text{O}_2$ terminated, which has been reported at room temperature,^{12–15} then O_2 annealing might etch the $\text{Al}-\text{O}_2$ surface layer to form single-height $\text{Al}-\text{O}_2$ islands on a $\text{La}-\text{O}$ base. The similarity in island structure before and after TiO_2 deposition [compare panels (a) and (b) in Figs. 1 and 2] reflects the approximate morphology and surface termination during TiO_2 growth, which occurred under oxygen rich conditions at 570 °C.

The observed TiO_2 nucleation at step edges, independent of the cation termination of the upper or lower terrace, implies that Ti prefers attaching to undercoordinated surface oxygen species at the steps (see Fig. 4), independent of the cation or number of oxygen atoms in the adjacent terrace. The question then arises as to why we observe subsequent growth of TiO_2 across both $\text{La}-\text{O}$ and $\text{Al}-\text{O}_2$ terraces with roughly equal probability.

The anatase layer structure is close to that of the $\text{Al}-\text{O}_2$ layer, with a small buckling to adjust the bond length; we thus expect straightforward epitaxy on the $\text{La}-\text{O}$ termination. In bulk LAO, $\text{La}-\text{O}$ layers donate a formal charge of 0.5 to each adjacent $\text{Al}-\text{O}_2$ layer; donating this charge to a TiO_2 layer would result in a mixed valence $\text{Ti}^{3+/4+}$ structure with a conducting interface.⁶ Although we do not observe a significant Ti^{3+} contribution in XPS at the interface, we do observe sufficient conduction in our films for conductive tunneling at room temperature once the film has coalesced, indicating a possible mixed valence interface. It is also possible that substitution of La^{3+} or Al^{3+} in the TiO_2 layer could lead to electronic conductivity without Ti^{3+} .

The low-energy sites above an $\text{Al}-\text{O}_2$ termination accommodate only a single positive and negative ion, with a separation $\sim 40\%$ larger than the $\text{Al}-\text{O}$ (or $\text{Ti}-\text{O}$) spacing. One possible growth mode is substitution of Ti for surface Al, perhaps with compensating oxygen vacancies in the interface layers. The extensive partial oxidation of Ti metal in the absence of an O_2 flux [Fig. 3(c)] indicates that some substrate cation-oxygen bonds may be replaced by $\text{Ti}-\text{O}$ bonding. Substitution of Ti for Al would place the first TiO_2 layer in a more favorable site than would direct adsorption

on Al–O₂; replacement of half the Al³⁺ by Ti⁴⁺ would also compensate for the formal 0.5*e* normally supplied by the adjacent La–O layer.

After the TiO₂ films coalesce, memory of the initial nucleation is reflected in the domain structure of the anatase surface reconstruction. The average domain size in Fig. 2(c) is comparable to both the island width and the spacing between TiO₂ nuclei in Fig. 2(b). In bulk anatase, (001) layers alternate between Ti–O bonds parallel to [100] and to [010] (see Fig. 4), so that the 1×4 reconstruction rotates by 90° and translates between adjacent terraces. The symmetry of both the La–O and Al–O₂ surface terminations of LAO(001) is such that [100] and [010] orientations of TiO₂ molecules would nucleate with equal probability.

The pattern of TiO₂ domains observed in Fig. 2(c) likely has three causes: (1) TiO₂ domains nucleated at 90° to each other on the same substrate terrace; (2) TiO₂ domains nucleating independently, parallel to each other, on adjacent substrate terraces; and (3) single-crystal TiO₂ domains containing a surface step that rotates the domain by 90°. These would result in adjacent rotated domains having the same height, heights differing by *d*_{LAO}, or heights differing by *d*_{TiO₂}, respectively. Our data are consistent with all three processes occurring, though it is not possible to decouple the last two within our experimental resolution.

V. SUMMARY

In summary, we have shown that annealing LaAlO₃(001) substrates in 5×10⁻⁵ torr of molecular O₂ and subsequently heating to 400 °C in UHV produces a surface consisting of one base termination (either La–O or Al–O₂) with about half the surface covered by single-layer high islands of the alternate surface termination. Alternating surface terminations has minimal effect on nucleation and growth of the single metal oxide TiO₂. Epitaxial anatase uniformly covers both terminations, in ~10 nm domains with two orthogonal surface layer orientations. The TiO₂ nucleates near steps, likely at undercoordinated oxygen sites.

ACKNOWLEDGMENTS

This work is supported by NSF Grant No. ECS 0224138 and M. J. Murdock Charitable Trust. One of the authors (D.A.S.) further acknowledges support from UW-PNNL Joint Institute for Nanoscience research award. Another author (T.O.) acknowledges support from the Center for Nanotechnology University Initiative Fund of the University of Washington. The authors acknowledge S. A. Chambers for fruitful discussions and sample standards. The authors further acknowledge F. S. Ohuchi for insightful suggestions.

- ¹R. W. Simon, C. E. Platt, A. E. Lee, G. S. Lee, K. P. Daly, M. S. Wire, and J. A. Luine, *Appl. Phys. Lett.* **57**, 1351 (1990).
- ²R. Brown, V. Pendrick, D. Kalokitis, and B. H. T. Chai, *Appl. Phys. Lett.* **57**, 1351 (1990).
- ³M. V. Jacob, J. Mazierska, N. Savvides, S. Ohshima, and S. Oikawa, *Physica C* **372–376**, 474 (2002).
- ⁴T. Stelzner, H. Schneidewind, and G. Bruchlos, *IEEE Trans. Appl. Supercond.* **13**, 2766 (2003).
- ⁵D.-W. Kim, D.-H. Kim, B.-S. Kang, T. W. Noh, D. R. Lee, and K.-B. Lee, *Appl. Phys. Lett.* **74**, 2176 (1999).
- ⁶A. Ohtomo and H. Y. Hwang, *Nature (London)* **427**, 423 (2004).
- ⁷Y. Matsumoto *et al.*, *Science* **291**, 854 (2001).
- ⁸S. A. Chambers, T. Droubay, C. M. Wang, A. S. Lee, R. F. C. Farrow, L. Folks, V. Deline, and S. Anders, *Appl. Phys. Lett.* **82**, 1257 (2003).
- ⁹J.-Y. Kim *et al.*, *Phys. Rev. Lett.* **90**, 017401 (2003).
- ¹⁰S. R. Shinde *et al.*, *Phys. Rev. B* **67**, 115211 (2003).
- ¹¹M. Murakami *et al.*, *Phys. Rev. Lett.* **78**, 2664 (2001).
- ¹²J.-P. Jacobs, M. A. S. Miguel, and L. J. Álvarez, *J. Mol. Struct.* **390**, 193 (1997).
- ¹³J.-P. Jacobs, M. A. S. Miguel, J. E. Sánchez-Sánchez, and L. J. Álvarez, *Surf. Sci.* **389**, L1147 (1997).
- ¹⁴P. A. W. van der Heide and J. W. Rabalais, *Chem. Phys. Lett.* **297**, 350 (1998).
- ¹⁵J. Yao, P. B. Miguel, S. S. Perry, D. Marton, and J. W. Rabalais, *J. Chem. Phys.* **108**, 1645 (1998).
- ¹⁶H. Kawanowa, H. Ozawa, M. Ohtsuki, Y. Gotoh, and R. Souda, *Surf. Sci.* **506**, 87 (2002).
- ¹⁷G. S. Herman, M. R. Sievers, and Y. Gao, *Phys. Rev. Lett.* **84**, 3354 (2000).
- ¹⁸Y. Liang, S. Gan, S. Chambers, and E. Altman, *Phys. Rev. B* **63**, 235402 (2001).
- ¹⁹M. Lazzeri and A. Selloni, *Phys. Rev. Lett.* **87**, 266105 (2001).
- ²⁰R. E. Tanner, Y. Liang, and E. Altman, *Surf. Sci.* **506**, 251 (2002).
- ²¹F. M. F. de Groot, J. C. Fuggle, B. T. Thole, and G. A. Sawatzky, *Phys. Rev. B* **41**, 928 (1990).
- ²²J. P. Crocombette and F. Jollet, *J. Phys.: Condens. Matter* **6**, 10811 (1994).
- ²³G. van der Laan, *Phys. Rev. B* **41**, 12366 (1990).
- ²⁴R. Ruus, A. Kikas, A. Ausmees, E. Nõmmiste, J. Aarik, A. Aidla, T. Uustare, and I. Martinson, *Solid State Commun.* **104**, 199 (1997).